Applied Energy 263 (2020) 114613

Contents lists available at ScienceDirect

Applied Energy

journal homepage: www.elsevier.com/locate/apenergy

An integrated blockchain-based energy management platform with bilateral trading for microgrid communities

Gijs van Leeuwen*, Tarek AlSkaif, Madeleine Gibescu, Wilfried van Sark

Copernicus Institute of Sustainable Development, Utrecht University (UU), Utrecht, the Netherlands

HIGHLIGHTS

- Optimal power flow and trading are combined in a single optimization problem.
- A real dataset from a prosumer community in Amsterdam is used.
- The role of a smart contract as a virtual aggregator is described in a detailed manner.
- Import cost reductions of up to 34.9% are found for the combined model.
- The combined model shows 50% reduced peak energy imports.

ARTICLE INFO

Keywords:
Microgrids
Distributed energy resources
Decentralized optimization
Optimal power flow
Local electricity markets
Blockchain
Smart contracts

ABSTRACT

In this paper, an integrated blockchain-based energy management platform is proposed that optimizes energy flows in a microgrid whilst implementing a bilateral trading mechanism. Physical constraints in the microgrid are respected by formulating an Optimal Power Flow (OPF) problem, which is combined with a bilateral trading mechanism in a single optimization problem. The Alternating Direction Method of Multipliers (ADMM) is used to decompose the problem to enable distributed optimization and a smart contract is used as a virtual aggregator. This eliminates the need for a third-party coordinating entity. The smart contract fulfills several functions, including distribution of data to all participants and executing part of the ADMM algorithm. The model is run using actual data from a prosumer community in Amsterdam and several scenarios of the model are tested to evaluate the impact of combining physical constraints and trading on social welfare of the community and scheduling of energy flows. The scenario variants are trade-only, where only a trading mechanism is implemented, grid-only where only OPF optimization is implemented and a combined scenario where both are implemented. Results are compared with a baseline scenario. Simulation results show that import costs of the whole community are reduced by 34.9% as compared to a baseline scenario, and total energy import quantities are reduced by 15%. Total social welfare is found to be highest without a trading mechanism, however this platform is only viable when all costs are equally shared between all households. Furthermore, peak imports are reduced by over 50% in scenarios including grid constraints.

1. Introduction

1.1. Background

The global need to mitigate CO_2 has led to an increased development and adoption of renewable energy generation technologies such as solar Photovoltaics (PV), as well as an electrification of various energy technologies that are traditionally based on fossil fuels, such as Electric Vehicles (EV) [1]. These and other Distributed Energy Resources (DER) are likely to be situated increasingly in the fringes of the Low Voltage (LV) distribution network where grid infrastructure may not be properly equipped to facilitate this [2]. It will be required to strengthen the grid physically or install more advanced control systems to enable bidirectional flow of electricity. Grid coordination in general will become much more complex [3].

Whilst the technical challenges are considerable, opportunities may also arise for citizens. Already, the increasing adoption of residential solar PV has led to an increase in the number of prosumers in the

* Corresponding author.
E-mail addresses: g.e.vanleeuwen2@students.uu.nl (G. van Leeuwen), t.a.alskaif@uu.nl (T. AlSkaif), m.gibescu@uu.nl (M. Gibescu), w.g.j.h.m.vansark@uu.nl (W. van Sark).

https://doi.org/10.1016/j.apenergy.2020.114613
Received 13 October 2019; Received in revised form 17 January 2020; Accepted 4 February 2020

Nomenclature

Abbreviations

AC	Alternating Current
ADMM	Alternating Direction Method of Multipliers
BS	Baseline summer scenario
BW	Baseline winter scenario
DER	Distributed Energy Resource
EV	Electric Vehicle
FiT	Feed-in-Tariff
GS	Grid-only summer scenario
GW	Grid-only winter scenario
HEMS	Home Energy Management System
ICT	Information and Communication Technology
LV	Low Voltage
OPF	Optimal Power Flow
P2P	Peer-to-Peer
PV	Photovoltaics
SOC	Second Order Cone
TGS	Trade-grid combined summer scenario
TGW	Trade-grid combined winter scenario
TS	Trade-only summer scenario
TW	Trade-only winter scenario

Parameters

$\mathbf{\Gamma}^{\mathrm{b,rel}}$	Relative willingness to buy
$\mathbf{\Gamma}^{\mathrm{s,rel}}$	Relative willingness to sell
$\boldsymbol{\sigma}$	The smart contract
$\boldsymbol{P}^{\mathrm{l}}$	Fixed real power load matrix
$\boldsymbol{P}^{\mathrm{net}}$	Net electricity budget matrix
$\boldsymbol{P}^{\mathrm{pv}}$	PV generation matrix
$\eta_{\mathrm{c}}^{\mathrm{b}}$	Battery charging efficiency
$\eta_{\mathrm{d}}^{\mathrm{b}}$	Battery discharging efficiency
η^{ev}	EV charging efficiency
κ_t	Costs of grid electricity [€/ kWh]
λ	Blockchain network adress
ω	Binary EV scheduling parameter
ϕ	Penalty parameter for trading mechanism
ρ	Penalty parameter for grid constraints
E^{ev}	Average daily charging demand [kWh]
Γ	Bilateral trading coefficient matrix
p^{l}	Fixed real power load [kWh]
p^{pv}	PV power generation [kWh]
q^{l}	Fixed reactive power load [kWh]
r	Resistance [Ω]
T	Number of timesteps
x	Reactance [Ω]

Sets

$\mathcal{A}$	Set of assets
$\mathcal{M}$	Set of trade partners
$\mathcal{N}$	Set of nodes
θ	Set of constructor variables
x_l	Set of local private variables
	Set of local coupling variables
x_g	Set of global variables

Variables

$\boldsymbol{D}$	Trading quantity matrix
ν	Squared voltage [V^2]
ψ	Squared current [A^2]
ξ	Price of trading and dual variable [€/ kWh]
C^{g}	Total costs of external grid imports [€]
e^{b}	Battery state of charge [kWh]
k_g	Number of corresponding local variables
P	Real power flow [kWh]
p	Net real power flow [kWh]
p^{g}	Real power imported from external grid [kWh]
p^{bc}	Battery charging power [kWh]
p^{bd}	Battery discharging power [kWh]
p^{b}	Net battery power generation [kWh]
p^{ev}	Real power consumption of EV [kWh]
Q	Reactive power flow [kWh]
q	Net reactive power [kWh]
q^{g}	Reactive power generation [kWh]
r_{grid}	Primal residual for grid constraints
r_{trade}	Primal residual for trading mechanism
S	Complex power flow [kWh]
s_{grid}	Dual residual for grid constraints
s_{trade}	Dual residual for trading mechanism
y	Dual variable for grid constraints

electricity market [4]. In various countries, Feed-In-Tariffs (FiTs) are in place to allow prosumers to sell energy back to the utility grid for a fixed price [5], and in the Netherlands net-metering policy is being phased out in favour of FiT [6]. Whilst Fit do provide a solution, it will be financially and energetically more efficient to maximize self-consumption by optimizing local use of energy [1]. This can be enabled by the deployment of energy storage systems [7,8] and schedulable electrical appliances or EVs that are configured to operate or charge at times when generation exceeds consumption [9]. Other solutions involve coordination at the community-level, such as novel types of consumer-centric electricity markets, where prosumers can trade or share energy between them [10,11]. These new types of markets are called Peer-To-Peer (P2P) markets [12]. P2P markets may be designed to prioritize the wellbeing of the participating individuals by providing maximum individual freedom, financial independence and privacy, or alternatively they may focus on the welfare of the community as whole, where participants may choose to share access to a common resource and aim to achieve a common goal such as total welfare maximization or autonomy [12]. P2P markets are now starting to emerge in the energy sector [13]. This can be recognized in the rise of community-based energy collectives [10,14–16].

The evolution of the electricity grid is enabled by several advancements in ICT technology. First of all, recent years have seen a large increase in the number of installed smart metering systems in Europe [4]. Analysis of data provided by these meters enables further energy management solutions and smart optimization of energy flows [17]. Expanding on a smart metering system is the home energy management system (HEMS). A HEMS is a system that is capable of balancing power usage in the household by measuring and controlling the operation of all connected electrical assets in a household [9].

Furthermore, digital platform technologies have shown their disruptive potential in several sectors. Such platforms may raise privacy issues when the platform being utilized is owned by a self-interested third party [18]. The algorithms that run the functionality of the platform are often not transparent for users, and they may be vulnerable to cyberattacks and tampering. The recent emergence of blockchain technology may provide a solution to these problems [18,19]. A blockchain is a type of distributed ledger technology that is used to connect a large number of anonymous nodes without the need for a central controlling agent. Blockchain technology utilizes a consensus

mechanism to ensure security of the network and allows participants to store and share data in a secure and verifiable manner, even when the identity and trustworthiness of other peers is unknown. Information is stored in sets of data called blocks and verified using cryptographic hashes. Participants can join or leave the blockchain network at any moment without impacting the operation of the system significantly and it is extremely difficult for external attackers to gain control of the blockchain. The clearest application for blockchain has proved to be verification of ownership, as is the case with cryptocurrency [20], but distributed computation between all connected devices is also possible. Extension of a blockchain with smart contract technology expands the utility even further and enables smart optimization in the energy sector [18,21].

1.2. Literature Review

Most of the work that is considered here can be categorised under the term “transactive energy” [22]. Transactive systems attain global goals through interactive and networked cooperation of independent and primarily self-interested actors. A precursor to transactive energy systems can be recognized in demand response programmes, which mainly provide financial incentives for consumers to withdraw energy from the grid during off-peak hours [23,24]. The work in [25] shows that the fundamental difference between demand side management and transactive energy is that the latter also manages the supply of energy. Transactive energy systems may focus on either the economic or engineering layer of the system [22], but ultimately the development of practical applications requires alignment and integration of business plans and engineering techniques, which is a considerable challenge. The various layers of a transactive energy system are also emphasised in [13] which distinguishes the four layers of the physical grid, ICT, control and market. In this section, relevant literature for the physical, economic and information (ICT) layer are reviewed. Furthermore, the literature for distributed optimization algorithms is reviewed.

In the physical grid, the optimal injections and withdrawals must be found while respecting physical constraints. A common way of doing this is formulating an Optimal Power Flow (OPF) problem [26]. The objective of an OPF problem is typically to minimize operation costs. OPF is a mathematical optimization problem that finds the optimal power injection levels and derives branch power flows and voltage levels in the process. OPF problems can be solved for both DC and AC systems and many scientific studies have recently used OPF in a microgrid context [27–30]. For instance, one particularly interesting study implements an AC-OPF problem on a blockchain platform for decentralized optimization [28]. The work in [30] designs a blockchain-assisted energy crowdsourcing system where the crowdsourcer manages the network and requests tasks from prosumers who could also trade energy within the distribution network.

In the economic layer, two categories of market structures can be distinguished [15]. On the one hand there is the full P2P market, where trades are conducted bilaterally and there is no centralized supervision. Maximum independence, freedom and anonymity are guaranteed in a full P2P market [12]. Full P2P markets in the energy sector have been explored in various recent studies [31,32]. One iconic study from the Brooklyn microgrid [33] has implemented a P2P trading scheme in a real physical microgrid. Supply and demand bids in this study are matched using a conventional merit-order dispatch. The second category of market structures is the energy collective or community based market. In this system, the interest of the group is paramount, and individual agents may sacrifice some of their own profits and interest for the collective social welfare. The work in [34] proposes a model where energy collectives may decide upon different goals, including total welfare maximization or autonomy from the external grid. In [35], a scenario where energy is shared in a microgrid that includes batteries is investigated and shows benefits for individuals as well as the community as a whole. Recently, a unified prosumer P2P market model has been formulated in [36]. This scheme may be operated with both bilateral trades and a centralized pool market, and provides an option for participants to declare preferred trading partners by including a trading penalty. A bilateral trading mechanism may provide benefits over the use of locational marginal prices, which have been used in other studies [37,28], since it provides participants with an extra degree of freedom and control over their trading. It can also be used to enable product differentiation, for example in [38].

In the information layer, the application of blockchain technology in the energy sector has been rapidly gaining attention from the scientific community. A large number of studies and initiatives about the use of blockchain in the energy sector are surveyed [18] and blockchain is seen as particularly promising in the area of P2P trading and decentralized energy management, since through blockchain a large number of self-interested actors can be connected and coordinated. The overall conclusion in this study is that blockchains may provide clear benefits to energy system operations, markets and consumers. The case study of the Brooklyn microgrid employs a blockchain network to connect participants [33], and shows that a blockchain can be successfully used to implement local electricity markets. The work in [28] expands on this by employing smart contracts on the blockchain network to enable decentralized optimization of an OPF problem without a central coordinator.

In the domain of distributed optimization algorithms there are several options that may be used to solve an OPF problem or ensure market clearance. A review of six decentralized algorithms that are suitable for this purpose, most notably the Alternating Direction Method of Multipliers (ADMM), is conducted in [27]. ADMM has seen the most extensive application in decentralized energy platforms. The ADMM algorithm is well suited to distributed convex optimization and operates by allowing decomposition of a global optimization problem into several sub-problems. The sub-problems are solved in parallel and their solutions are coordinated to come to a solution of the global problem [39]. An OPF problem can be decomposed into sub-problems using ADMM, where every sub-problem is related to a small part of the grid. ADMM has been used extensively in recent studies to decompose OPF problems [28,40,41]. Similarly, ADMM can also be utilized to decompose a market clearing problem, where a common approach is to formulate the global optimization problem as a maximization of total social welfare [15,36,34].

1.3. Contributions

The aim of this study is to design an integrated energy management platform that implements solutions in the physical, economic and information layers. The goal of the platform is to optimize the flow of electricity in a distributed manner in a realistic microgrid configuration which features a number of households with access to a variety of DERs. OPF is used to determine power flows in the physical layer, and a bilateral trading mechanism is implemented in the economic layer. The bilateral trading mechanism provides households with greater control over their trading, and allows them to indicate preferred trading partners. It could also be used to enable product differentiation. In the information layer, the model is implemented on a blockchain network with a smart contract acting as a virtual aggregator. Fig. 1 shows the structure of the platform. The goal of optimization is to maximize total social welfare of all connected actors where the highest social welfare is typically represented by the minimal financial costs. The ADMM algorithm is used to solve the optimization problem in a distributed manner. The modelled platform is intended to provide a high degree of independence, privacy and transparence by the implementation on the blockchain network, as well as personal choice and freedom through bilateral trading. Although similar models have been developed before, as can be seen from Section 1.2, there are several novel contributions that this study intends to make.

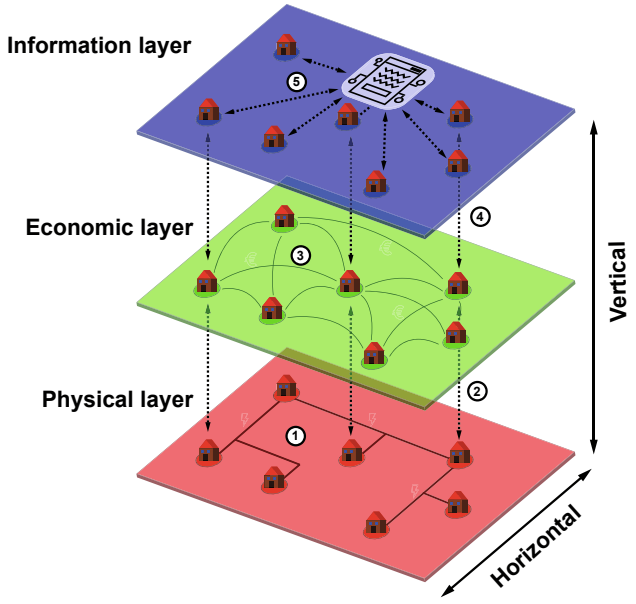

Fig. 1. Illustration of the different layers of the proposed model and the interaction between them. (1) In the physical layer, power flows in the horizontal dimension between households through grid connections. (2) Information is exchanged in the vertical dimension between the economic and the physical layer. (3) In the economic layer, a trading mechanism is used to enable monetary compensation for power injections and withdrawals into/from the grid. (4) Information is exchanged between the information layer and the layers below. (5) The households send their locally calculated optimal schemes for the economic and physical layers to the smart contract.

1. Firstly, an AC-OPF problem is combined with a bilateral trading mechanism in a single optimization problem. To the authors' best knowledge this is the first time such a model is proposed.
2. Secondly, the implementation on the blockchain platform and specifically the role of the smart contract are described in a detailed manner. The smart contract fulfills the role of a virtual aggregator and executes several parts of the ADMM algorithm.
3. Thirdly, the model is being tested using a dataset from a real prosumer community in Amsterdam. This will give a more realistic view than the use of constructed data.

The paper is structured as follows. The setup of the model is presented in Section 2, where the general layout and setup of the grid and households are presented in Section 2.1. The centralized formulations of the OPF problem and trading mechanism are given in Sections 2.2 and 2.3, respectively, and the decentralized formulations of both are given in Section 2.4. The blockchain implementation is detailed in Section 2.5 and the configuration of the numerical analysis can be found in Section 2.6. The results are given in Section 3, and a discussion of these results is found in Section 4. Finally, the study is concluded in Section 5.

2. Model setup

The proposed platform is designed to function on a microgrid network that features consumers and prosumers with access to privately owned EVs, solar PV installations and battery systems. It functions as a day-ahead energy scheduling platform, and every prosumer household is considered as a separate node on the network. Households are able to trade their excess or deficit electricity budget between them and can indicate preferred trading partners by assigning bilateral trading coefficients to individual trades. Participants act in a mostly self-interested way, but also contribute to the balancing and management of the microgrid, which may involve some sacrifice of self-benefit. The combined optimization problem is formulated in a distributed form using the ADMM algorithm. Finally, the distributed optimization problem is implemented on a private blockchain test network by porting part of the algorithm's functionality to a smart contract. Fig. 1 shows the layered structure of the model. Different versions of the platform are tested that include and exclude the grid constraints and the trading mechanism. These different scenarios are detailed in Section 2.6. A comparison is also made with a baseline scenario where there is only passive interaction between households and the external grid.

2.1. Grid and household setup

The microgrid considered in this study is modelled as a radial Low Voltage (LV) network over a number of timesteps T, indexed by $t = 0, 1, ..., T$. It can be represented by a set of nodes $\mathcal{N}$, indexed by $i = 0, 1, ..., n$, and connecting lines $\mathcal{L}$, indexed by $l = 0, 1, ..., L$. Node 0 is designated as the root node. A node in $\mathcal{N}$ can be either referred to with its index number i or as a neighbouring node of another node j. In this relationship, j is defined as the node that is closer (i.e. fewer connecting lines) to the root node. As such, j is called the parent node of i, and can be referred to as $\pi(i)$. In similar fashion, node i is called the k-th child node of j, and can be referred to as $\delta_k(j)$. Due to the radial nature of the network, every node only has one parent node. A node can have multiple children, and the set of children nodes of node j is referred to as $\delta(j)$, indexed by $k = 0, 1, ..., c$. For simplicity, every line in $\mathcal{L}$ is designated to have the same index number as the connected child node. In every line i, the complex impedance is denoted as $z_i = r_i + ix_i$, where r and x are the resistance and reactance in the line.

All households in $\mathcal{N}$ have access to a connection to the grid. Power is fed into and withdrawn from the microgrid through these connections. Power is imported from the utility grid at the root of the network, and is designated as $p^{g}_{i,t}$. The costs of withdrawing power from the external grid at time t is represented by κ_t. The cost function for each household i in timestep t can then be formulated as:

$$C^{g}_{i,t}(p^{g}_{i,t}) = \kappa_t p^{g}_{i,t}, \quad \forall \ i, t. \tag{1}$$

Every household also has a fixed real power load $p^{l}_{i,t}$ and fixed reactive power load $q^{l}_{i,t}$ that are uncontrollable. Controllable reactive power generation $q^{g}_{i,t}$ is assumed to be available to those households that have access to solar PV [42]. The generation of real and reactive power is constrained within upper and lower limits as follows:

$$\underline{p}^{g}_{i} \leqslant p^{g}_{i,t} \leqslant \overline{p}^{g}_{i}, \quad \forall \ i, t, \tag{2}$$

$$\underline{q}^{g}_{i} \leqslant q^{g}_{i,t} \leqslant \overline{q}^{g}_{i}, \quad \forall \ i, t. \tag{3}$$

Other assets that are available only to some households but not others include solar PV, EV and battery systems. The availability of solar PV yields a fixed, uncontrollable power generation $p^{pv}_{i,t}$. The availability of EV and battery systems yields additional constraints. An EV is considered to be a shiftable load where both the time and quantity of the charging power $p^{ev}_{i,t}$ can be controlled. Total daily charge must equal the daily charging demand E^{ev}_{i}, as can be seen in Eq. (4) and the EV charging efficiency is given by η^{ev}. Furthermore, EV charging rate is constrained within upper and lower charging limits. Vehicle-to-Grid technology is out of the scope of this research. A binary parameter $\omega_{i,t}$ is used in Eq. (5) to indicate the timeslots at which the EV charging can be scheduled. It should be noted that this modelling of EV charging patterns is simplified and not a fully accurate representation of real behaviour. Still, for the current purposes of evaluating performance of the proposed platform with the presence of flexible load, the current formulation is viable and sufficient.

$$\sum_{t=0}^{T} \eta^{ev} p^{ev}_{i,t} \Delta t = E^{ev}_{i}, \quad \forall \ i, \tag{4}$$

$$\omega_{i,t}\underline{p}^{\text{ev}} \leqslant p_{i,t}^{\text{ev}} \leqslant \omega_{i,t}\overline{p}^{\text{ev}}, \quad \forall\ i,\ t. \tag{5}$$

For the battery, the net battery power $p_{i,t}^{\text{b}}$ is defined as the difference between the discharging power $p_{i,t}^{\text{bd}}$ and the charging power $p_{i,t}^{\text{bc}}$, as follows:

$$p_{i,t}^{\text{b}} = p_{i,t}^{\text{bd}} - p_{i,t}^{\text{bc}}, \quad \forall\ i,\ t. \tag{6}$$

The state of charge of the battery is represented by $e_{i,t}^{\text{b}}$, and the efficiency of charging and discharging are represented by $\eta_{\text{c}}^{\text{b}}$, $\eta_{\text{d}}^{\text{b}}$, respectively. $e_{i,t}^{\text{b}}$ is determined as follows:

$$e_{i,t}^{\text{b}} = e_{i,t-1}^{\text{b}} + \left(\eta_{\text{c}}^{\text{b}} p_{i,t}^{\text{bc}} - \frac{p_{i,t}^{\text{bd}}}{\eta_{\text{d}}^{\text{b}}}\right)\Delta(t), \quad \forall\ i,\ t. \tag{7}$$

$p_{i,t}^{\text{bd}}$, $p_{i,t}^{\text{bc}}$ and $e_{i,t}^{\text{b}}$ are all constrained within upper and lower limits.

Finally, every household has a connection to the microgrid, allowing for withdrawal and injection of real and reactive power. Net power injections into the microgrid are designated as $p_{i,t}$ and $q_{i,t}$, with positive values representing injection and negative values representing withdrawal. $p_{i,t}$ and $q_{i,t}$ are calculated as follows:

$$p_{i,t} = p_{i,t}^{\text{g}} + p_{i,t}^{\text{pv}} + p_{i,t}^{\text{b}} - p_{i,t}^{\text{l}} - p_{i,t}^{\text{ev}}, \quad \forall\ i,\ t, \tag{8}$$

$$q_{i,t} = q_{i,t}^{\text{g}} - q_{i,t}^{\text{l}}, \quad \forall\ i,\ t. \tag{9}$$

2.2. AC-OPF problem

For the complex power flow through line i at time t, $P_{i,t}$ and $Q_{i,t}$ represent the real and reactive power flow. The convention is adopted that positive values represent power flow from i to j. The squared voltage at node i is represented by $\nu_{i,t} = v_{i,t}^2$ and the squared current is represented by $\psi_{i,t} = I_{i,t}^2$. These quantities can be related by adopting the branch flow model for modelling the AC power flow in a single phase radial network [26,43]. The branch flow model is then relaxed using a Second Order Cone (SOC) convex relaxation [26,44]. The following equations from the branch flow model are considered:

$$p_{i,t} = P_{i,t} - \sum_{k\in\delta_i} P_{k,t} - r_i\psi_{i,t}, \quad \forall\ i,\ t, \tag{10a}$$

$$q_{i,t} = Q_{i,t} - \sum_{k\in\delta_i} Q_{k,t} - x_i\psi_{i,t}, \quad \forall\ i,\ t, \tag{10b}$$

$$\nu_{i,t} = \nu_{j,t} + 2(r_i P_{i,t} + x_i Q_{i,t}) - \psi_{i,t}(r_i^2 + x_i^2), \quad \forall\ i,\ t, \tag{10c}$$

$$\psi_{i,t} = \frac{P_{i,t}^2 + Q_{i,t}^2}{\nu_{i,t}}, \quad \forall\ i,\ t. \tag{10d}$$

Eq. (10d) is a non-convex constraint, and is relaxed to the following inequality [44]:

$$P_{i,t}^2 + Q_{i,t}^2 \leqslant \psi_{i,t}\nu_{i,t}, \quad \forall\ i,\ t. \tag{11}$$

The squared voltage $\nu_{i,t}$ is to be constrained within upper and lower limits, which are defined as 5% above and below a nominally defined voltage.

The optimization objective of the AC-OPF problem is to minimize total costs of grid imports for every household. It is formulated as follows:

$$\begin{aligned} &\text{minimize} && \textstyle\sum_{t=0}^{T}\sum_{i=0}^{N} C_{i,t}(p_{i,t}^{\text{g}}), \\ &\text{subject to} && (4) - (11). \end{aligned} \tag{12}$$

2.3. Trading Mechanism

For the trading mechanism, the unified prosumer market proposed in [36] is adopted. The unified model provides options for implementing either a pool market model or a bilateral trading system. For the purposes of this study the bilateral trading form is used, which allows the designation of a bilateral trading coefficient to every individual trade. Bilateral trading coefficient values can be decided by the household owners, and can thus be used to indicate preferred trading partners and enable product differentiation. Every node in $\mathcal{N}$ is considered to be a separate rational, non-strategic market agent. In the unified prosumer market model, costs for every separate agent are minimized across their set of connected assets. This includes the costs of trading with the other participants. It is formulated as follows:

$$\text{min.} \quad \sum_{t=0}^{T}\sum_{i=0}^{\mathcal{N}}\left[\sum_{a=1}^{\mathcal{A}} f_{i,t}^{a}(p_{i,t}^{a}) + \sum_{j=0}^{\mathcal{M}} \gamma_{ij,t}\left|d_{ij,t}\right|\right], \tag{13a}$$

$$\text{s. t.} \quad \boldsymbol{D}_t = -\boldsymbol{D}_t^{\text{T}} \quad [\Xi_t] \qquad \forall\ t, \tag{13b}$$

$$\sum_{a=1}^{\mathcal{A}} p_{i,t}^{a} = \sum_{j=0}^{\mathcal{M}} d_{ij,t} \qquad \forall\ i,\ t, \tag{13c}$$

$$p_{i,t}^{a} \in \mathcal{P}_{i,t}^{a} \qquad \forall\ a,\ i. \tag{13d}$$

In this formulation, $\mathcal{A}$ indexed by a represents the set of assets of agent i, and $\mathcal{M}$ indexed by j represents the set of trading partners of agent i. $f_{i,t}^{a}$ represents the cost function of asset a as a function of the power set point $p_{i,t}^{a}$. $\gamma_{ij,t}$ represents the bilateral trading coefficient imposed by agent i on the trade between agents i and j, and $d_{ij,t}$ is the quantity of electricity traded between agents i and j. The matrix $\boldsymbol{D}$ contains the quantities of all trades, and the associated dual variable matrix Ξ contains the prices of all trades. Set $\mathcal{P}_{i,t}^{a}$ contains the feasible set of power set points of i at t. Constraint Eq. (13b) enforces reciprocity of trade quantities, and reciprocity of trading prices Ξ is also implicitly enforced by this constraint as it is the dual variable. Constraint Eq. (13c) ensures that the sum of all power generated by agent i equals the sum of the quantities of all trades conducted.

2.4. Decentralized formulation

2.4.1. General Consensus ADMM

In order to optimize in a distributed manner, the general consensus optimization form of the ADMM algorithm is used. In this section only, the formulation from [39] is used for the general form consensus problem. In its general form, it is written as follows:

$$\text{min.} \quad \sum_{i=0}^{\mathcal{N}} f_i(x_i), \qquad \forall\ i, \tag{14a}$$

$$\text{s. t.} \quad x_i - \widetilde{z}_i = 0, \qquad \forall\ i. \tag{14b}$$

From this, the augmented Lagrangian of this problem is formulated as:

$$L_\rho\left(x, z, y\right) = \sum_{i=0}^{\mathcal{N}}\left(f_i(x_i) + y_i^{\text{T}}\left(x_i - \widetilde{z}_i\right) + \left(\rho/2\right)\|x_i - \widetilde{z}_i\|_2^2\right), \tag{15}$$

where y represents the dual variable, and ρ represents the penalty parameter (i.e. the step size) which is predefined. In Eq. (15), minimizing the second and third terms enforces constraint Eq. (14b). Eq. (15) is solved through a series of iterative steps, which are formulated as:

$$x_i^{k+1} = \underset{x_i}{\text{argmin}}\left(f_i(x_i) + y_i^{k\,\text{T}}\left(x_i - \widetilde{z}_i^{k}\right) + \left(\rho/2\right)\|x_i - \widetilde{z}_i^{k}\|_2^2\right), \tag{16a}$$

$$z_g^{k+1} = \left(1/k_g\right)\sum_{\mathcal{G}(i,c)=g}(x_i^{k+1})_c, \tag{16b}$$

$$y_i^{k+1} = y_i^{k} + \rho(x_i^{k+1} - \widetilde{z}_i^{k+1}). \tag{16c}$$

Eq. (16b) is essentially an averaging of all local variable components to retrieve the corresponding global variable component. The ADMM

algorithm will iterate through the steps until the convergence conditions are met. These conditions are evaluated through the primal and dual residual values r^k and s^k, which are defined as follows:

$$r^k = x_i^k - \tilde{z}_i^k, \tag{17a}$$

$$s^k = z_g^k - z_g^{k-1}. \tag{17b}$$

The convergence conditions are then defined as:

$$\|r^k\|_2 \leqslant \epsilon_p, \tag{18a}$$

$$\|s^k\|_2 \leqslant \epsilon_d. \tag{18b}$$

In Eqs. (18a) and (18b), ϵ_p and ϵ_d are the allowed tolerances for the primal and dual residuals, respectively, which are typically assigned a low value in the range of $10^{-2} - 10^{-3}$. Besides meeting the convergence conditions, the execution of and ADMM algorithm is also typically assigned a maximum number of iterations after which execution of the algorithm will end.

2.4.2. ADMM + AC-OPF

The AC-OPF of Eq. (12) is reformulated using the general consensus form ADMM. The global optimization problem is decomposed into a set of subproblems where every node $i \in \mathcal{N}$ solves its own local subproblem using its own set of local variables x_i. In this set of local variables, the subset of local private variables $(x_l)_i := [p_i, p_i^{\mathrm{g}}, q_i, q_i^{\mathrm{g}}, \psi_i, p_i^{\mathrm{b}}, p_i^{\mathrm{bc}}, p_i^{dc}, e_i^{\mathrm{b}}, p_i^{\mathrm{ev}}]$ generally contains the variables pertaining to local energy infrastructure and the set of local coupling variables $(x_u)_i := [P_i, Q_i, v_i, P_{\delta(i)}, Q_{\delta(i)}, v_{\pi(i)}]$ generally contains the variables pertaining to its set of branch flow equations. The set of global variables is denoted as $z_g := [P, Q, v]$. Fig. 2 shows how the locally calculated coupling variables correspond to the global variables in the present OPF problem. The steps of the ADMM algorithm are executed according to Eqs. (16a)–(16c), as follows:

$$\underset{p_{i,t}^{\mathrm{g}}}{\operatorname{argmin}} \; C_{i,t}(p_{i,t}^{\mathrm{g}}) + y_i^{k^{\mathrm{T}}}\left(x_i - \tilde{z}_i^k\right) + \left(\rho/2\right)\|x_i - \tilde{z}_i^k\|_2^2, \tag{19a}$$

s. t. (4) − (11),

$$z_g^{k+1} = \left(1/k_g\right) \sum_{\mathcal{G}(i,c)=g} (x_i^{k+1})_c, \tag{19b}$$

$$y_i^{k+1} = y_i^k + \rho(x_i^{k+1} - \tilde{z}_i^{k+1}). \tag{19c}$$

2.4.3. ADMM + Trading mechanism

As for the OPF problem, the centralized optimization problem Eq. (13a) is decomposed into subproblems where every agent solves their corresponding subproblem. Every agent will determine their own local trading schedule $\boldsymbol{D}$, which is treated as a coupling variable that corresponds to the global variable $\boldsymbol{C}$. Following [36], $(\boldsymbol{C} - \boldsymbol{C}^{\mathrm{T}})/2 = \boldsymbol{D}$ is defined as the average of the trading quantity proposed by agent i to agent j and the trading quantity proposed by agent j to agent i. By using this consensus constraint, the fully decentralized augmented Lagrangian for bilateral trading can be formulated as follows, according to [36]:

$$(p_i^{\mathrm{g}}, D_i)^{k+1} = \underset{p_i^{\mathrm{g}}, D_i}{\operatorname{argmin}} \; \sum_{t=0}^{\mathcal{T}} \Big[C_{i,t}^{\mathrm{g}}(p_{i,t}^{\mathrm{g}}) + \sum_{j=0}^{\mathcal{M}} [\gamma_{ij,t} |d_{ij,t}^{k+1}| + \tag{20a}$$

$$(\phi/2)\left(\frac{d_{ij,t}^k - d_{ji,t}^k}{2} - d_{ij,t}^{k+1} + \xi_{ij,t}^k/\phi\right)^2 \Big] \Big]$$

subject to: (20b)

$$p_{i,t} = \sum_{j=0}^{\mathcal{M}} d_{ij,t},$$

(4) − (8).

In this formulation the penalty parameter is represented by ϕ to distinguish it from the penalty parameter in Eq. (19a)–(19c). Dual variable ξ, representing the price of trading, being updated in the next step:

$$\xi_{ij,t}^{k+1} = \xi_{ij,t}^k - \rho\left(d_{ij,t}^{k+1} + d_{ji,t}^{k+1}\right)/2. \tag{21}$$

2.4.4. Combined formulation

As stated, the main contribution of this study is the combination of an OPF problem with a trading mechanism in a single distributed optimization problem. This leads to a fully decentralized algorithm that achieves maximum total social welfare by minimizing both grid import costs and trading costs for every agent $i \in \mathcal{N}$ separately and in parallel while respecting global grid constraints and balancing supply and demand. The fully decentralized algorithm consists of several iterative steps. First, the local optimization problem is solved by agent i:

$$(x_i, \boldsymbol{D}_i)^{k+1} = \underset{x_i, T_i}{\operatorname{argmin}} \; \sum_{t=0}^{T} [C_{i,t}^{\mathrm{g}}(p_{i,t}^{\mathrm{g}}) + y_{i,t}^{k^{\mathrm{T}}}(x_{i,t} - \tilde{z}_{i,t}^k) + (\rho/2)\|x_{i,t} - \tilde{z}_{i,t}^k\|_2^2 + \sum_{j=0}^{\mathcal{M}} [\gamma_{ij,t} |d_{ij,t}^{k+1}| + (\phi/2)\left(\frac{d_{ij,t}^k - d_{ji,t}^k}{2} - d_{ij,t} + \left(\xi_{ij,t}^k/\phi\right)^2\right)\Big]\Big]$$

subject to (4) − (11), (20b) (22)

It can be recognized that two separate penalty parameters are used, ρ for the grid constraints and ϕ for the trading mechanism. Since the only cost-generating asset in this setup is the external grid connection, $\sum_{a=1}^{\mathcal{A}} f_{i,t}^a(p_{i,t}^a)$ is replaced by $C_{i,t}^{\mathrm{g}}(p_{i,t}^{\mathrm{g}})$, which is the cost function of the external grid connection. In this first step, agent i calculates both the set of local variables x_i and the optimal trading schedule $\boldsymbol{D}$ for every timestep. In the next step, the global variables z_g are calculated:

$$z_g^{k+1} := \left(1/k_g\right) \sum_{\mathcal{G}(i,c)=g} (x_i^{k+1})_c. \tag{23}$$

In the third step, dual variables y and ξ are updated by every agent:

$$\xi_{ij,t}^{k+1} = \xi_{ij,t}^k - \phi\left(d_{ij,t}^{k+1} + d_{ji,t}^{k+1}\right)/2, \quad \forall \; j, t, \tag{24a}$$

$$y_i^{k+1} = y_i^k + \rho(x_i^{k+1} - \tilde{z}_i^{k+1}). \tag{24b}$$

After every iteration, separate sets of residuals for grid constraints and trading are calculated as follows:

$$r_{\mathrm{grid}}^{k+1} = \sum_{i=0}^{\mathcal{N}} x_i^k - \tilde{z}_i^k, \tag{25a}$$

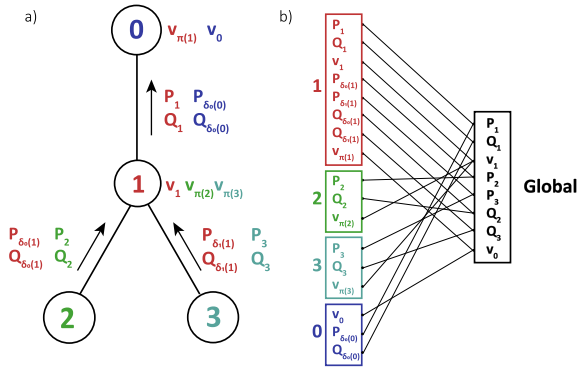

Fig. 2. An illustration of the coupling between local and global variables in the ADMM-based general form consensus method for the OPF problem in a 4-nodes network.

$$s_{\text{grid}}^{k+1} = \sum_{i=0}^{\mathcal{N}} \tilde{z}_i^k - \tilde{z}_i^{k-1}, \tag{25b}$$

$$r_{\text{trade}}^{k+1} = \sum_{i=0}^{\mathcal{N}} \sum_{t=0}^{T} \sum_{j=0}^{\mathcal{M}} (d_{ij,t}^{k+1} + d_{ji,t}^{k+1})^2, \tag{25c}$$

$$s_{\text{trade}}^{k+1} = \sum_{i=0}^{\mathcal{N}} \sum_{t=0}^{T} \sum_{j=0}^{\mathcal{M}} (d_{ij,t}^{k+1} - d_{ij,t}^{k})^2. \tag{25d}$$

2.5. Blockchain implementation

By adopting blockchain and smart contracts technology the proposed distributed algorithm can be executed in a secure, verifiable manner that ensures independence and anonimity of the market participants. In such a setup, the role of the smart contract is essential. A smart contract is a piece of computer code that is deployed on the blockchain and can execute certain functions when called upon by other nodes [19,21]. The smart contract takes over the function of this central aggregator, thus effectively functioning as a virtual aggregator. In this role, the smart contract performs several types of functions:

1. Executing parts of the ADMM algorithm
2. Exchanging information with other nodes
3. Giving permission to other nodes to proceed with the next operation.

Various steps in the ADMM algorithm are distinguished where these functions are executed. In this work the smart contract is written in the Solidity language and the other files that are run locally are written in Python. Web3.py [45] is used to communicate between Python and the contract, and the local optimization problems are solved using the Cvxpy package [46]. The blockchain network is set up by running a local Ethereum node with Ganache-cli [47]. It should be noted that the proposed blockchain setup is not assessed for efficiency of communication, security, execution speed and energy consumption.

Upon setting up the blockchain network every node i is assigned a personal account with address λ_i, and the smart contract σ is assigned an account λ_σ. The contract is deployed to the network using a set of constructor variables $\theta := [n, \rho, \phi, \epsilon_p^{\text{g}}, \epsilon_d^{\text{g}}, \epsilon_p^{t}, \epsilon_d^{t}, \mu]$ that configure the integrated ADMM algorithm. The variable μ represents the maximum number of iterations, n represents the total number of nodes on the network. It can be noted that it is not required to pass any information on the network topology. As the contract is deployed, the bytecode of the contract's contents ABI_σ are generated. λ_σ and ABI_σ must be known by all other nodes to allow them to interact with the contract.

In the execution of the ADMM algorithm on the blockchain network for the integrated model there are several steps that can be distinguished, which are visualised in Fig. 3.

1. In step 1, i connects to σ by using the adress λ_σ and bytecode ABI_σ. This action only has to be performed once.
2. In step 2 a new round of optimization starts for the next day, and all nodes will declare their participation by passing i, the number of the node, and $\pi(i)$ and $\delta(i)$, the numbers of the parent and child nodes. Also, the nodes will retrieve θ from the contract to configure the local optimization problem. σ keeps track of participating nodes using a counter and when all n nodes have declared participation, the nodes will proceed to solve their local optimization problem.
3. When local optimization Eq. (22) is complete, the nodes send their sets of coupling variables $(x_u)_i$ and their set of trade bids d_i to the smart contract which will keep track using a counter. When all nodes submitted their coupling variables, one node is configured to call the z-update step function, which will make the contract execute Eq. (23) of ADMM. Note that the set of trade bids contains the optimally calculated trading quantities for all trading partners and all timesteps. For the trading portion, the only role of the smart contract is to gather all trade bids and distribute them to the respective trading partners.
4. When the z-update step is complete, the nodes will retrieve the recalculated global variables $\tilde{z}_i$ as well as the trade bids of their trading partners d_j. The nodes will form their full trading quantity matrix $d_{ij,t}$ and calculate their local penalty values as in Eq. (24a) and Eq. (24b). The nodes will also calculate the partial residual values as in Eqs. (25a)–(25d) for their local problem.
5. The nodes send the partial residuals $r_{grid,i}$, $s_{grid,i}$, $r_{trade,i}$, $s_{trade,i}$ to the contract, which initiates a counter and sums all partial residuals upon completion to receive the global residuals. The nodes periodically call checking functions to check for completion.
6. The nodes retrieve the global residual values r_{grid}, s_{grid}, r_{trade}, s_{trade} and evaluate the converge conditions. If the conditions are not satisfied, go back to step 3) and repeat.

If at any point in the algorithm a node fails to provide the necessary information, the system will timeout since full optimization needs all the information from every node to complete. It can be recognized that very little sensitive information is shared by the nodes with the contract. All information regarding the local energy infrastructure (i.e. local private variables $(x_l)_i$) remains private: only data on power flows in adjacent lines is shared, as well as residual values and trade bids. This information is stored on the smart contract, and not accessible by any other nodes on the network. Furthermore, it can be recognized that full network topology is not explicitly stated anywhere. Every node must only know its parent and children. As for the end-user interaction with the blockchain network, the HEMS could perform virtually all of the required actions. In the configuration of the optimization problem and connection to the blockchain network, all communication with the network can be automated in the HEMS, requiring no knowledge of the blockchain's operation on the part of the end-user.

2.6. Numerical analysis

For the fixed real power load and solar generation data, actual data from the East Harbour Prosumers Community [48] in Amsterdam is used. The fixed reactive power load $q_{i,t}^l$ is assumed to be proportional to − 1/10th of the fixed real power load $p_{i,t}^l$. For the topology of the radial microgrid, the network of [49] is used. The topology is indicated in Fig. 4. It can be recognized that 11 households in the network are prosumers and that 8 households are owners of an EV. For grid electricity withdrawals, a time-of-use price signal κ_t is used from the day-ahead market clearing prices of the European Power Exchange (EPEX) Netherlands [50]. Based on average daily distance travelled in the Netherlands by EV, the average EV daily charging demand (E_{ev}) is set at 7.06 kWh [51,52]. The charging hours ω_i are pre-defined, with some

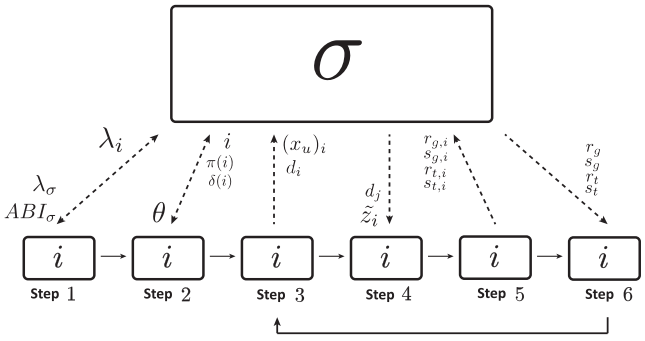

Fig. 3. A flowchart showing the interaction between the smart contract σ and node i in the steps of the ADMM algorithm. The g and t subscripts indicate grid and trade residuals, respectively.

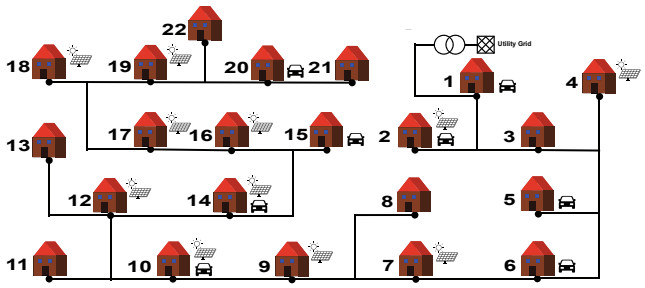

Fig. 4. Topology of the considered microgrid. Owners of EV and PV are indicated.

households preferring to charge during the day and others during the night. The charging efficiency of EV is set at 90%, and the battery efficiency is set at 95%.

For every day, the bilateral trading coefficients are pre-determined for every household based on their fixed real power consumption and solar PV generation data. It should be emphasized that in a real setup the values of the coefficients are decided by the household owners to indicate preferred trading partners or allow for product differentiation. It is assumed that the willingness to trade of a household i in any timestep t is proportional to the magnitude of their expected deficit/surplus $p^{l}_{i,t} - p^{\text{pv}}_{i,t}$. It is assumed that households with an expected surplus budget are more likely to trade with households that have an expected deficit and visa versa. In order to reflect these assumptions in the bilateral trading coefficients, several steps are taken.

First, the expected net budget matrix $\boldsymbol{P}^{\text{net}}$ is determined. Along the rows it contains all households and is indexed by i, and along the columns it contains all timesteps and is indexed by t. $\boldsymbol{P}^{\text{net}}$ is defined as:

$$\boldsymbol{P}^{\text{net}} = \boldsymbol{P}^{\text{pv}} - \boldsymbol{P}^{\text{l}} \tag{26}$$

where $\boldsymbol{P}^{\text{pv}}$ and $\boldsymbol{P}^{\text{l}}$ have the same dimensions as $\boldsymbol{P}^{\text{net}}$. From matrix $\boldsymbol{P}^{\text{net}}$, two new matrices $\boldsymbol{P}^{\text{buy}}$ and $\boldsymbol{P}^{\text{sell}}$ are defined. These matrices contain the amount of power that each household wants to sell or buy in every timestep. The elements from these matrices are determined as follows:

$$p^{\text{buy}}_{i,t} = \begin{cases} 0 & \text{if} \quad p^{net}_{i,t} \geqslant 0 \\ p^{net}_{i,t} & \text{if} \quad p^{net}_{i,t} < 0 \end{cases} \tag{27a}$$

$$p^{\text{sell}}_{i,t} = \begin{cases} p^{\text{net}}_{i,t} & \text{if} \quad p^{net}_{i,t} > 0 \\ 0 & \text{if} \quad p^{net}_{i,t} \leqslant 0 \end{cases} \tag{27b}$$

From these matrices, two column vectors $\overline{P}^{\text{buy}}_{\text{max}}$ and $\overline{P}^{\text{sell}}_{\text{max}}$ are defined. Each element of these vectors represents the maximum value in the corresponding row of the matrices $\boldsymbol{P}^{\text{buy}}$ and $\boldsymbol{P}^{\text{sell}}$. This means that these vectors contain the maximum deficit and surplus budget of every household across all timesteps. $\boldsymbol{P}^{\text{buy}}$ and $\boldsymbol{P}^{\text{sell}}$ are then normalized as:

$$\boldsymbol{\Gamma}^{\text{b,rel}} = \frac{\chi}{2} \frac{\boldsymbol{P}^{\text{buy}}}{\overline{P}^{\text{buy}}_{\text{max}}} \tag{28a}$$

$$\boldsymbol{\Gamma}^{\text{s,rel}} = \frac{\chi}{2} \frac{\boldsymbol{P}^{\text{sell}}}{\overline{P}^{\text{sell}}_{\text{max}}} \tag{28b}$$

Matrices $\boldsymbol{\Gamma}^{\text{b,rel}}$ and $\boldsymbol{\Gamma}^{\text{s,rel}}$ represent the relative willingness of households to buy or sell electricity. Parameter χ represents the maximum, baseline value for bilateral trading coefficients. From matrices $\boldsymbol{\Gamma}^{\text{b,rel}}$ and $\boldsymbol{\Gamma}^{\text{s,rel}}$, the final 3D matrix of bilateral trading coefficients $\boldsymbol{\Gamma}$ is defined as follows:

$$\gamma_{ij,t} = \begin{cases} \chi & \text{if } \gamma^{\text{s,rel}}_{i,t}, \gamma^{\text{s,rel}}_{j,t} > 0 \\ \chi & \text{if } \gamma^{\text{b,rel}}_{i,t}, \gamma^{\text{b,rel}}_{j,t} > 0 \\ \chi - (\gamma^{\text{b,rel}}_{i,t} + \gamma^{\text{b,rel}}_{j,t} + \gamma^{\text{s,rel}}_{i,t} + \gamma^{\text{s,rel}}_{j,t}) & \text{otherwise} \end{cases} \tag{29}$$

At the maximum value of $\gamma_{ij,t} = \chi$, nodes i and j are considered very unlikely trading partners. In the present study, χ is set at 10, meaning that all bilateral trading coefficients have a value of anywhere between 0 and 10.

Table 1
Considered scenarios for numerical evaluation.

Scenario	Abbreviation
Baseline, summer	BS
Baseline, winter	BW
Trade only, summer	TS
Trade only, winter	TW
Grid only, summer	GS
Grid only, winter	GW
Grid + Trade, summer	TGS
Grid + trade, winter	TGW

In order to evaluate the impact of including the bilateral trading mechanism and grid constraints on social welfare and scheduling of power flows and bilateral trades, several scenarios are compared where these different parts of the model are included and excluded. A baseline scenario will also be analysed, where there is no microgrid and households only interact with the external grid. In all scenarios, prosumers are able to feed their excess electricity budget into the grid for 50% of the electricity price at that time. The scenarios are run for one week in summer (21–28 June 2018) and one week in winter (21–28 December 2018) to evaluate performance in both seasons. The different scenarios are shown in Table 1. The trade-only scenarios execute the optimization problem as in Eq. (20b), grid-only scenarios execute as in Eqs. (19a)–(19c), the combined scenarios execute as in Eq. 22. In the grid-only scenarios, there is no cost on the exchange of energy so that the impact of including the bilateral trading mechanism can be more clearly assessed in isolation.

3. Results

The objective of this study is to assess the performance of the integrated model and to compare it with a baseline scenario. This performance is assessed with regard to economic indicators and the scheduling of power flows.

The economic performance parameters represent financial costs for the households. Table 2 shows values for total social welfare across the entire week. In this table, a comparison is made between total prosumer costs and total consumer costs. Furthermore, Fig. 5 shows the price of electricity throughout the entire week, both for trading, grid imports and grid feed-in.

Results for power imported across the week, in total and at peak hours, are found in Table 3.

Based on the results shown in the figures and tables, a comparison can be made between the different scenarios for every performance category. Building on this, the respective benefits and downsides of the scenarios can be discussed, as well as their applicability in real-life communities. This analysis is provided in Section 4.

3.1. Economic indicators

Looking at the results for total community-wide costs in Table 2, it can be recognized that in summer the BS scenario yields the highest costs (rounded numbers) at 182 euros. The GS scenario results in the lowest costs at around 83 euros, which is 45% of the baseline scenario. Total costs in the TS and TGS scenarios are only slightly lower than BS at around 168 euros, respectively. When regarding only external grid imports, which includes compensation from feed-in, the GS scenario is still the cheapest at 83 euros, but the difference between the BS scenario on the one hand and the TS and TGS scenarios on the other is much larger, with the BS coming in at 182 euros and the TS and TGS yielding 130 and 118 euros, respectively. Differences between the

Table 2
Numerical results for economic indicators. All costs are summed over the entire week and over all households. Prosumer and consumer costs are summed over all prosumer and consumer households, respectively. Relative costs are compared to the baseline scenarios, the values of which are set at 100%. For the trade costs, the values of the trade-only scenarios is set at 100%.

	Summer				Winter			
Scenario	BS	GS	TS	TGS	BW	GW	TW	TGW
Prosumer import costs (Eur)	90.17	53.46	70.84	60.06	150.82	126.56	132.76	136.05
Consumer import costs (Eur)	92.23	30.01	59.59	58.74	151.44	118.19	148.02	147.32
Prosumer trade costs (Eur)	–	–	−37.40	−49.37	–	–	0	0
Consumer trade costs (Eur)	–	–	37.40	49.37	–	–	0	0
Total prosumer costs (Eur)	90.17	53.46	33.44	10.69	150.82	126.56	132.76	136.05
Total consumer costs (Eur)	92.23	30.01	96.99	108.11	151.44	118.19	148.02	147.32
Total import costs (Eur)	182.40	83.47	130.43	118.8	302.26	244.75	280.78	283.37
Total trade costs (Eur)	–	–	37.40	49.37	–	–	0	0
Total costs (Eur)	182.40	83.47	167.83	168.17	302.26	244.75	280.78	283.37
Relative prosumer import costs	100%	59.3%	78.6%	66.6%	100%	83.9%	88.0%	90.2%
Relative consumer import costs	100%	32.5%	64.6%	63.7%	100%	78.0%	97.7%	92.2%
Relative prosumer trade costs	–	–	100%	132.0%	–	–	100%	100%
Relative consumer trade costs	–	–	100%	132.0%	–	–	100%	100%
Relative total prosumer costs	100%	59.3%	36.8%	11.8%	100%	83.9%	88.0%	90.2%
Relative total consumer costs	100%	32.5%	105.2%	117.2%	100%	78.0%	97.7%	92.2%
Relative total import costs	100%	45.8%	71.5%	65.1%	100%	80.1%	92.9%	93.8%
Relative total trade costs	–	–	100%	132.0%	–	–	100%	100%
Relative total costs	100%	45.8%	92.0%	92.2%	100%	80.1%	92.9%	93.8%

scenarios are larger when distinguishing prosumers and consumers. In the BS scenario, prosumer costs are almost the same as consumer costs around 90 euros. In the GS scenario, prosumer costs are 54 euros, which is higher than consumer costs at 30 euros. In both trading scenarios however, the difference between prosumers and consumers is much larger, with the total consumer costs being around 3 times higher than the prosumer costs in the TS scenario, and almost 10 times higher in the TGS scenario. In the winter scenarios, differences between the scenarios are much smaller, and give the same overall picture. Looking at Fig. 5, it can be recognized that during daytime hours, when trading is most likely to take place, the average internal trading price is lower than the price of grid imports yet higher than the compensation for grid feed-in. It can also be recognized that the TS and TGS scenarios yield similar results for the price of internal trading, as well as the TW and TGW scenarios. For the TG and TGW scenarios, the trading price is not between feed-in and withdrawal prices, but these data should not be considered meaningful or reliable since there is next to no trading happening in these scenarios. The boxplots in Fig. 7 show the distribution of total costs data for households in every scenario, split up for prosumers and consumers. It can be seen that in the GS scenario there is the least variation, both for consumer and prosumer households. In the trading scenarios, the variation is significantly larger, with the variation in TS being somewhat larger than in TGS.

Table 3
Numerical results for energy consumption. Grid imports and the energy exchanged are summed over the entire week and over all households. Peak hours are defined as 6–9am in the morning and 5–8 pm in the evening, and peak imports are summed over all peak hours for all days and all households. Relative values are compared to the baseline scenarios, the values of which are set at 100%.

	Summer				Winter			
Scenario	BS	GS	TS	TGS	BW	GW	TW	TGW
Total local energy exchange (kWh)	–	495	291	468	–	52	5	17
Total imports (kWh)	999	788	895	856	2638	2333	2530	2455
Peak imports (kWh)	731	273	620	302	1199	843	1140	876
Ratio of peak/total imports	0.73	0.34	0.69	0.35	0.45	0.36	0.45	0.35

3.2. Scheduling indicators

Table 3 shows the results for energy imports and energy exchanged in all scenarios. The GS scenario yields the highest local energy exchange at 495 kWh as there is no price on trading. The TGS scenario yields a similar amount at 468 kWh, with the TS being the lowest at 291 kWh of traded energy. For the winter scenarios, very little exchange is occuring as there is almost no excess solar electricity. For energy

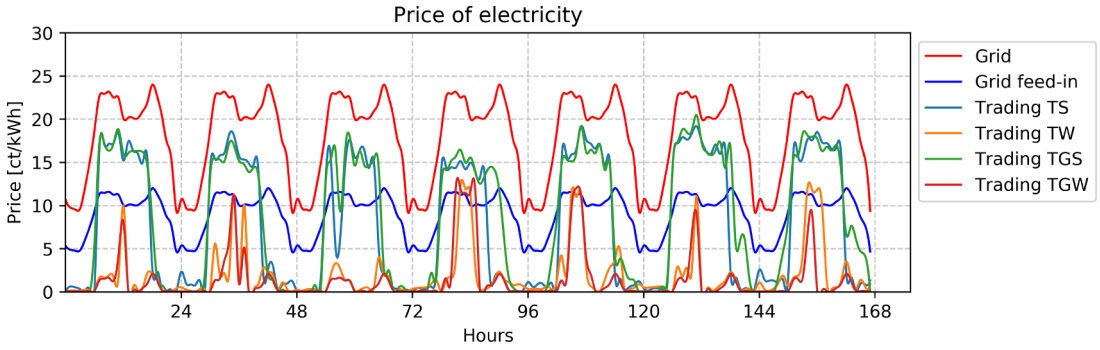

Fig. 5. The price of electricity in the different scenarios.

imports, the BS scenario shows a higher result than the other summer scenarios at a total withdrawal of 999 kWh. The GS scenario has the lowest consumption at 788 kWh, and the TS and TGS scenarios show values of 895 and 856 kWh, respectively. There is a large difference in peak imports, with the TS and BS scenario showing values of 70% of total imports, whereas in the GS and TGS scenarios the peak imports are around 35% of the total. In the winter scenarios again differences are smaller, there is only a noticable variation with the peak imports where again GW and TGW scenarios yield the lowest values. Looking at Fig. 6, which shows the power exchanged throughout the first day of the four summer scenarios, it can be recognized that there is no import peak at peak hours in the GS and TGS scenarios. Furthermore, it appears that power flows are smoother and more consistent throughout the day. In the scenarios that include trading, this trading is limited during daytime hours when there is an excess of PV. In the GS scenario, there is some more exchange happening during other hours as well as it is free.

4. Discussion

As has been shown in Section 3, results in winter are very similar for all scenarios. This makes sense as there is very little excess PV electricity during this time of year, which means that the microgrid is relatively inactive as most PV electricity is self-consumed directly. Therefore, further discussion of the results will focus on the results of the summer scenarios.

4.1. Discussion of economic and scheduling results

Out of the GS, TS and TGS scenarios, the GS scenario shows favourable results for total social welfare. Total costs in this scenario are considerably lower than for the other scenarios, which means that total social welfare is the highest. This can simply be explained by the absence of trading costs as energy is exchanged for free. GS scenario is also cheapest when considering only import costs however, and so it appears that the absence of a trading mechanism allows the microgrid to function at maximum efficiency. When comparing TS and TGS scenarios, the inclusion of the microgrid constraints in TGS results in a slightly higher import costs than in TS. This can be explained by efficiency losses which are not considered in the TS scenario. Although the total energy imports in Table 3 are fairly close together for the three scenarios, the real difference shows in the peak imports, where the GS and TGS show peak imports that are less than half that of the TS and BS scenarios. It appears that inclusion of physical network constraints in the optimization problem means that the algorithm will avoid using the grid excessively during peak hours, not just because of cost incentives, but also because of possible congestion issues. From Fig. 6, it can be seen that overall power flows are smoother in the G scenarios. In the TS and BS scenarios, this management is left to the DSO. Furthermore, when comparing the amount of energy that is traded in the TS and TGS scenarios, it appears that the TGS scenario allows for a larger quantity of energy to be traded at a similar price as the TS scenario. Possibly this is a result of more local trading during peak hours to compensate for the lower external grid imports.

4.2. Inequality between prosumers and consumers

Looking at the differences between total prosumer and consumer costs, the inequality is significantly larger in the trading scenarios than in the others. This makes sense given that this difference is primarily a result of the trading. When considering only import costs, it appears that consumers benefit more than prosumers from the proposed setup as compared to the BS scenario. Still, it is clear that owners of PV

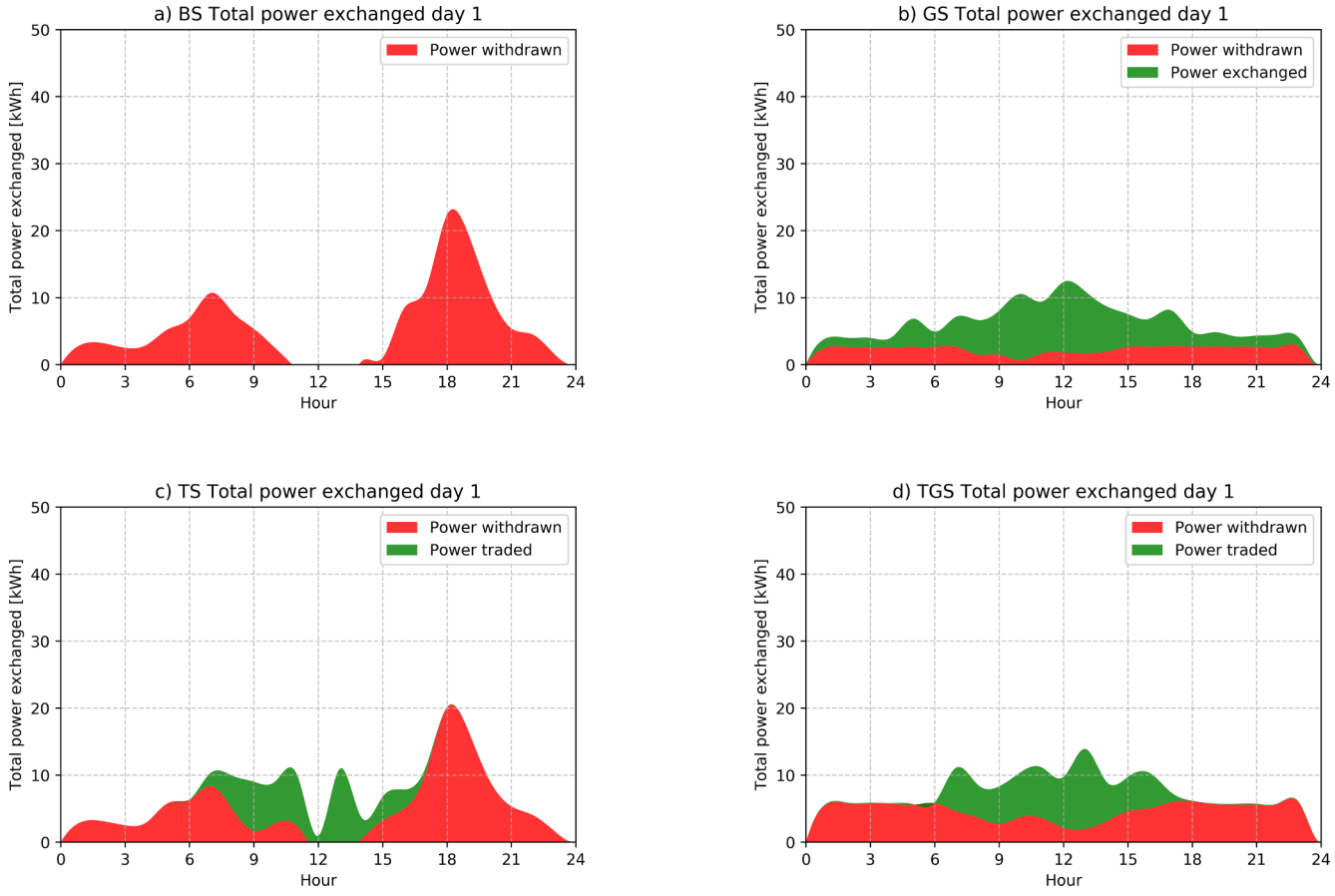

Fig. 6. Power exchanged in all nodes during the first day of the summer scenarios. Magnitudes are summed over all nodes.

benefit of their investment through the trading. The GS scenario is most beneficial for consumers, yet prosumers still benefit as compared to the TS and TGS scenarios. When comparing the TS and TGS scenarios the figures are similar. Prosumers benefit more in the TGS scenario because of increased trading, and for the same reason consumers pay a bit more. This increased benefit is not a result of the trading price, which is similar in both scenarios as can be recognized from Fig. 5, but of increased trading volume, as can be seen in Table 3. Fig. 7 shows the spread in costs for all households. Similar to the other results, the GS scenario shows the lowest spread and the TS and TGS show a larger, yet similar spread. TGS spread appears to be somewhat smaller. In the winter scenarios the difference between consumers and prosumers is much smaller as there is very little trading happening.

4.3. Real life application

4.3.1. Baseline and grid-only scenarios

First of all, the BS scenario represents a situation that is similar to the present situation in the distribution grid in some countries. There is no cooperation between households on any level, and prosumers may dispose of their excess PV-generated electricity by feeding it into the grid. A financial compensation is offered to them in the form of FiTs, and battery storage systems are only for private use. Consumers are completely reliant on their energy service providers to provide them with energy. Also, this scenario requires the DSO to monitor and distribute energy in the grid and ensure that all physical constraints are respected. Given the expected increase in DER adoption [3,52,53], this task will become more and more complex. Furthermore, considering the expected abolishment of net metering [6], prosumers must find other ways to optimally benefits from their installed PV systems. Coupled with the developments discussed in Section 1, it seems likely that the system configuration represented in the baseline scenarios will increasingly be replaced by alternative systems. This is reinforced by the result from this study that the BS scenario yields the highest total costs and grid imports of all summer scenarios. Of the other scenarios, the GS scenario yields the highest social welfare and lowest peak imports. In fact, peak imports are just over one-third of the BS scenario. This can be very beneficial for the DSO. This scenario can be conceptualized as a microgrid community that shares energy between community members. The GS scenario appears to only be viable when costs of grid imports are fairly shared across all members of the network or when the exchange of power is valued using for instance locational marginal prices, like in [37]. Furthermore, a way should be found to compensate investors of PV and batteries for their extra contribution to the total welfare of the community. This would require intensive cooperation between all participants on the network, and the resulting community would be akin to an energy collective as discussed in Section 1.2. In such a community, there would be no need for a trading mechanism since all households will act in the interest of the group.

4.3.2. Trading scenarios

When intensive cooperation is not possible and households act in a mostly self-interested manner, the inclusion of a trading mechanism can regulate cooperation whilst still ensuring maximization of total social welfare. The TS scenario seems viable when all participants on the network are primarily self-interested and little cooperation between them is possible or desirable. Such a network may be akin to a full P2P market as discussed in Section 1.2. The mechanism allows prosumers to benefits maximally from their PV and battery systems. The TGS scenario is similar to the TS scenario, except that grid management is adopted by the network participants. The largest benefit of this is a significant decrease in peak imports of over 50%. This can be very beneficial for the DSO. Furthermore, some efficiency losses from grid management are not included in the TS scenario because they are left to the DSO, meaning that in reality the energy consumption will be somewhat higher than the figures found here. It is also interesting that the inclusion of the OPF equations allows for more trading to take place in the TGS scenario (see Table 3 and Fig. 5), allowing participants to benefit more from the bilateral trading system that is in place. Monetarily speaking, prosumers do benefit more from TGS scenario as compared to consumers. As such, it is more heavily incentivized in the TGS scenario to have a PV installation than in the TS scenario.

4.4. Overall comparison

For social welfare, it appears that the best result is achieved without implementing a trading mechanism (GS scenario), and a combination of physical microgrid constraints and trading mechanism (TGS scenario) yields lowest social welfare. However, not implementing a trading system means that intensive cooperation between the households is required, and that participants cannot benefit from the options and freedom provided by the bilateral trading mechanism. Furthermore, the trading mechanism favours owners of PV, incentivizing adoption and investment of such rooftop systems. When considering the TS and TGS scenarios, social welfare results are similar, and the main benefit from the addition of the OPF problem appears to be strongly reduced peak imports, as well as a slightly reduced total imports. Increased trading volume in TGS is also beneficial. Comparing to the baseline scenario, the other three scenarios show considerable benefits, especially regarding the import costs. Trading costs are spent by individual households but the money remains within the community, thus arguable still benefiting the community as a whole. The TGS scenario shows lower import costs than the TS scenario at 35.4% lower than the baseline scenario, and peak imports are 60% lower than the baseline. Total imports are around 15% lower than in the baseline. Overall, it seems that applicability of the different scenarios in real life is dependent on the nature of the cooperation between the participants, as well as the cooperation between the community and the DSO. Given that the present study proposes a platform that is implemented on blockchain, it seems reasonable that adopters of such platforms hold independence, free choice and anonymity in high regard, which could make it feasible for them to adopt any of the platforms modelled in the different scenarios. A platform similar to the GS scenario would fit a situation where independence and welfare of the community as a whole are deemed important. In this case, individuals must be prepared to collaborate intensively to fairly share costs and take responsibility for microgrid management. The TS scenario seems to fit a community where participants prioritize individual choice, freedom and welfare and do no desire to be involved in local grid management. The TGS scenario represents a middle ground where extra responsibility is adopted for management of the microgrid, but where cooperation between

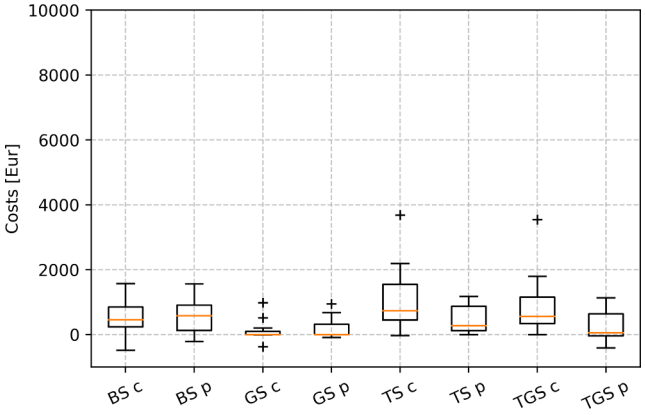

Fig. 7. Boxplot showing the total costs for households in all scenarios. These data are summed over the entire week. The 'c' and 'p' indicate data for consumer and prosumer households, respectively. Yellow lines indicate median values of the particular group. (For interpretation of the references to colour in this figure legend, the reader is referred to the web version of this article.)

participants is regulated by a trading mechanism.

4.5. The blockchain network and end-user interaction

It should be emphasized that the proposed model is intended to function on a private blockchain network, where all participants are known and accepted members of the community. In this case, it is not possible for just anyone to enter the network and participate. Particularly when the platform is implemented in a microgrid environment this is impossible since it would require that the new participant is physically connected to the microgrid: in a trade-only scenario, it would be possible to allow new participants as no physical connection is required, although this might have consequences for overall performance of the algorithm when the number of participants becomes too large. Regarding end-user interaction with the network, virtually none is required: almost all actions can be automated by the HEMS, where the local optimization problem and communication with the blockchain network are all performed by the HEMS. The only input that the end-user would need to pass to the HEMS would be the designated EV charging hours. The bilateral trading coefficients could either be determined manually by the end user, or, like shown in this study, automatically calculated.

4.6. Limitations

4.6.1. Structural limitations

First of all, the modelled platform is intended to function as a day-ahead optimization platform, meaning that outcomes are dependent on accuracy of PV generation and consumption forecasts. Regarding the implementation on blockchain, the suggested configuration has not been extensively tested for communication efficiency, security and execution speed, even though these are important factors. The aim of this study has been to provide a general framework for implementation and for using the smart contract. Regarding the development of the model, there are always inherent uncertainties in the software that is used, in this case Python, Cvxpy, Ganache-cli and Web3.py. Also, uncertainties are inherently present in the branch flow model and the ADMM algorithm, since a distributed optimization algorithm typically does not converge to exactly the same solution as a centralized algorithm. Furthermore, the proposed integrated model could benefits from a comprehensive sensitivity analysis to evaluate how the input parameters and setup of the two parts of the model affect performance and results in both categories.

4.6.2. Assumptions

Other important limitations arise from the assumptions that are made in the setup of the model. It has been assumed that all EVs have the same average charging demand and charging hours every day, which is not likely to occur in a real-life situation. Also, values have been assumed for the battery parameters, and assumptions have been made regarding the availability of reactive power generation and the topology of the grid. It is unclear whether varying the amount or distribution of DERs in the microgrid will severely affect the outcome, and the investment costs of the various assets has not been taken into account. For battery systems in particular, the investment costs can play a large role when making financial calculations in a model. Finally, the bilateral trading coefficients may have large impacts on the outcomes of the model. In this study, an effort has been made to set realistic values for the bilateral trading coefficients in a relatively straightforward manner based on the net power consumption in each timestep, but a more extensive modelling of prosumer market behaviour may provide further insights into the impact of the coefficient values.

5. Conclusions

This study has shown the modelling of an integrated blockchain-based energy management platform that respects physical microgrid constraints and implements a bilateral trading mechanism. The procedure of integrating the physical, economic and information layers in a single model has been shown in Section 2. As a first main contribution, the formulation of a distributed optimization problem that respects physical microgrid limitations through OPF and implements a bilateral trading mechanism has been detailed in Section 2.4.1. As a second main contribution, the implementation of the distributed algorithm on a blockchain network has been specified in Section 2.5. A smart contract can take on the role of virtual aggregator: Not only does it have to execute the consensus step from the ADMM algorithm, it also functions as a central agent for distributing required information and data to all other nodes. Several scenarios are defined, the setup of which has been detailed in Section 2.6. The results of running the scenarios have been shown in Section 3 and have been discussed in Section 4.

Although combining the trading mechanism and physical constraints yields a somewhat lower total social welfare, peak imports as well as grid import costs are reduced as compared to the trade-only scenario. The GS scenario, while showing the best results for social welfare, seems difficult to realize since intensive cooperation is required. Furthermore, it does not provide the benefits conferred by the bilateral trading mechanism. As such, it appears that there are considerable benefits to combining trading with physical constraints when designing energy optimization platforms, especially when comparing to the baseline scenario: Import costs are reduced by 34.9%, and peak import quantity is reduced by 60%. Regarding real-life applicability, it is argued that a trade-only scenario could represent full P2P type markets, whereas a grid-only scenario could represent an energy collective. The combined scenario could represent a middle-ground where several downsides of the other scenarios are mitigated. Research into the social acceptance of the different scenarios and actual wishes of participants could give further insights into the practical feasibility. The usefulness of the proposed model can be expanded in several ways. First of all, the model could be implemented on a live blockchain network to evaluate security, efficiency and execution speed in a real life situation. Furthermore, the sensitivity of modelling results to input parameters such as trading coefficients, investment costs and DER distribution could be explored. Also, a detailed techno-economic assessment could be carried out to evaluate social welfare over an extended period of time.

Declaration of Competing Interest

The authors declare that they have no known competing financial interests or personal relationships that could have appeared to influence the work reported in this paper.

Acknowledgements

This work is partly funded by the research project: ”A Blockchain-based platform for peer-to-peer energy transactions between Distributed Energy Resources (B-DER)”, Netherlands Enterprise Agency (RVO) within the Dutch Topsector Energy framework, project number: 1621404. The authors would like to thank the project partner Hugo Niesing at Resourcefully for sharing the data of the East Harbour Prosumer Community.

References

[1] Terlouw T, AlSkaif T, Bauer C, van Sark W. Optimal energy management in all-electric residential energy systems with heat and electricity storage. Appl Energy 2019;254:113580.
[2] Ipakchi A, Albuyeh F. Grid of the future. IEEE Power Energy Mag 2009;7(2):52–62. https://doi.org/10.1109/MPE.2008.931384.
[3] Farhangi H. Path of the smart grid. IEEE Power Energy Mag 2010;8(1):18–28. https://doi.org/10.1109/MPE.2009.934876.
[4] EURELECTRIC. Prosumers – an integral part of the power system and the market.

Eurelectric 2015(June):15. doi: D/2015/12.105/15 < http://www.eurelectric.org/media/178736/prosumers_an-integral_part_of_the_power_system_and_market_june_2015-2015-2110-0004-01-e.pdf > .
[5] Bakhtyar B, Fudholi A, Hassan K, Azam M, Lim CH, Chan NW, Sopian K. Review of CO2 price in Europe using feed-in tariff rates. Renew Sustain Energy Rev 2017; 69 (October 2015): 685–91. doi:https://doi.org/10.1016/j.rser.2016.11.146.
[6] G. of the Netherlands, Salderingsregeling verlengd tot 2023; 2019. https://www.rijksoverheid.nl/actueel/nieuws/2019/04/26/salderingsregeling-verlengd-tot-2023.
[7] Lüth A, Zepter JM, Crespo del Granado P, Egging R. Local electricity market designs for peer-to-peer trading: the role of battery flexibility. Appl Energy 2018;229(May):1233–43. https://doi.org/10.1016/j.apenergy.2018.08.004.
[8] Terlouw T, AlSkaif T, Bauer C, van Sark W. Multi-objective optimization of energy arbitrage in community energy storage systems using different battery technologies. Appl Energy 2019;239:356–72.
[9] AlSkaif T, Luna AC, Zapata MG, Guerrero JM, Bellalta B. Reputation-based joint scheduling of households appliances and storage in a microgrid with a shared battery. Energy Build 2017;138:228–39. https://doi.org/10.1016/j.enbuild.2016.12.050.
[10] Pinson P, Baroche T, Moret F, Sousa T, Sorin E, You S. The emergence of consumer-centric electricity markets. Distrib Utiliz 2017:1–5. http://pierrepinson.com/docs/pinsonetal17consumercentric.pdf.
[11] AlSkaif T, Zapata MG, Bellalta B, Nilsson A. A distributed power sharing framework among households in microgrids: a repeated game approach. Computing 2017;99(1):23–37. https://doi.org/10.1007/s00607-016-0504-y.
[12] Einav L, Farronato C, Levin J. Peer-to-Peer Markets. Annu Rev Econ 2016. https://doi.org/10.1146/annurev-economics-080315-015334.
[13] Zhang C, Wu J, Long C, Cheng M. Peer-to-peer energy trading in a microgrid. Appl Energy 2018;220:1–12. https://doi.org/10.1109/TSG.2013.2284664.
[14] Van Der Schoor T, Scholtens B. Power to the people: local community initiatives and the transition to sustainable energy. Renew Sustain Energy Rev 2015;43:666–75. https://doi.org/10.1016/j.rser.2014.10.089.
[15] Sousa T, Soares T, Pinson P, Moret F, Baroche T, Sorin E. Peer-to-peer and community-based markets: a comprehensive review. Renew Sustain Energy Rev 2019. https://doi.org/10.1016/j.rser.2019.01.036.
[16] Fleischhacker A, Lettner G, Schwabeneder D, Auer H. Portfolio optimization of energy communities to meet reductions in costs and emissions. Energy 2019. https://doi.org/10.1016/j.energy.2019.02.104.
[17] Ma Z, Xie J, Li H, Sun Q, Si Z, Zhang J, Guo J. The role of data analysis in the development of intelligent energy networks. IEEE Network 2017;31(5):88–95. https://doi.org/10.1109/MNET.2017.1600319.
[18] Andoni M, Robu V, Flynn D, Abram S, Geach D, Jenkins D, McCallum P, Peacock A. Blockchain technology in the energy sector: a systematic review of challenges and opportunities. Renew Sustain Energy Rev 2019. https://doi.org/10.1016/j.rser.2018.10.014.
[19] Yli-Huumo J, Deokyoon K, Choi S, Park S, Smolander K. Where is current research on blockchain technology? – a systematic review. PLoS ONE 10 (11). doi:https://doi.org/10.1371/journal.pone.0163477.
[20] Nakamoto S. Bitcoin; 2019. https://bitcoin.org/bitcoin.pdf.
[21] Wood G. Ethereum: a secure decentralised generalised transaction ledger, Ethereum Project Yellow Paper. https://ethereum.github.io/yellowpaper/paper.pdf.
[22] Hammerstrom D, Widergren S, Irwin C. Evaluating transactive systems. IEEE Electrification Mag 4:30–6. doi:https://doi.org/10.1109/MELE.2016.261418.
[23] Albadi MH, El-Saadany EF. A summary of demand response in electricity markets. Electric Power Syst Res 2008;78(11):1989–96. https://doi.org/10.1016/j.epsr.2008.04.002.
[24] Staats M, de Boer-Meulman P, van Sark W. Experimental determination of demand side management potential of wet appliances in the netherlands. Sustain Energy Grids Networks 9. doi:https://doi.org/10.1016/j.segan.2016.12.004.
[25] Chen S, Liu C-C. From demand resopnse to transactive energy: state of the art. J Mod Power Syst Clean Energy 2017;1(5):10–9. https://doi.org/10.1007/s40565-016-0256-x.
[26] Taylor JA. Convex optimization of power systems. Cambridge University Press 2015. https://doi.org/10.1017/CBO9781139924672. https://www.cambridge.org/core/product/identifier/9781139924672/type/book.
[27] Kargarian A, Mohammadi J, Member S, Guo J, Member S, Chakrabarti S, Member S, Barati M, Hug G, Member S, Kar S, Baldick R. Toward distributed/decentralized DC optimal power flow implementation in future electric power systems. IEEE Trans Smart Grid 2018;9(4):2574–94. https://doi.org/10.1109/TSG.2016.2614904.
[28] Münsing E, Mather J, Moura S. Blockchains for decentralized optimization of energy resources in microgrid networks. In: 2017 IEEE conference on Control Technology and Applications (CCTA), IEEE; 2017. p. 2164–71.
[29] Guerrero J, Chapman AC, Verbic G. Decentralized P2P energy trading under network constraints in a low-voltage network. IEEE Trans Smart Grid 2018. https://doi.org/10.1109/TSG.2018.2878445.
[30] Wang S, Taha A, Wang J, Kvaternik K, Hahn A. Energy crowdsourcing and peer-to-peer energy trading in blockchain-enabled smart grids. IEEE Trans Syst Man Cybernet: Syst. doi:arXiv:1901.02390 [cs.SY].
[31] Morstyn T, Teytelboym A, McCulloch MD. Bilateral contract networks for peer-to-peer energy trading. IEEE Trans Smart Grid 2019;10(2):2026–35. https://doi.org/10.1109/TSG.2017.2786668.
[32] Morstyn T, McCulloch M. Multi-class energy management for peer-to-peer energy trading driven by prosumer preferences. IEEE Trans Power Syst 2018. https://doi.org/10.1109/TPWRS.2018.2834472.
[33] Mengelkamp E, Gärttner J, Rock K, Kessler S, Orsini L, Weinhardt C. Designing microgrid energy markets: a case study: the brooklyn microgrid. Appl Energy 2018;210:870–80. https://doi.org/10.1016/j.apenergy.2017.06.054.
[34] Moret F, Pinson P. Energy collectives: a community and fairness based approach to future electricity markets. IEEE Trans Power Syst 2018:1–11. https://doi.org/10.1109/TPWRS.2018.2808961.
[35] Long C, Wu J, Zhou Y, Jenkins N. Peer-to-peer energy sharing through a two-stage aggregated battery control in a community Microgrid. Appl Energy 2018;226(May):261–76. https://doi.org/10.1016/j.apenergy.2018.05.097.
[36] Baroche T, Moret F, Pinson P. Prosumer markets: a unified formulation. In: IEEE PowerTech conference; 2019. p. 1–6.
[37] Kim B, Baldick R. IEEE Trans. Power Syst. 2000;15(2):599–604. https://doi.org/10.1109/59.867147.
[38] Sorin E, Bobo L, Pinson P. Consensus-based approach to peer-to-peer electricity markets with product differentiation. IEEE Trans Power Syst 2019;34(2):994–1004. https://doi.org/10.1109/TPWRS.2018.2872880.
[39] Boyd S. Distributed optimization and statistical learning via the alternating direction method of multipliers. Found Trends Mach Learn 2011;3(1):1–22. https://doi.org/10.1561/2200000016. arXiv:0307085.
[40] Kraning M, Chu E, Lavaei J, Boyd S. Message passing for dynamic network. Energy Manage 2012;1(2):70–122. arXiv:1204.1106.
[41] Erseghe T. Distributed optimal power flow using admm. IEEE Trans Power Syst 2014;29(5):2370–80. https://doi.org/10.1109/TPWRS.2014.2306495.
[42] Adhikari S, Li F. Coordinated v-f and p-q control of solar photovoltaic generators with mppt and battery storage in microgrids, IEEE Trans Smart Grid 5 (3). doi:https://doi.org/10.1109/TSG.2014.2301157.
[43] Baran ME, Wu FF. Optimal capacitor placement on radial distribution systems. IEEE Trans Power Deliv 1989;4(1):725–34.
[44] Low SH. Convex relaxation of optimal power flow-part i: formulations and equivalence. IEEE Trans Control Network Syst 2014;1(1):15–27.
[45] Ethereum, Web3.py; 2019. https://github.com/ethereum/web3.py.
[46] Diamond S, Boyd S. Cvxpy: A python-embedded modeling language for convex optimization. J Mach Learn Res 2016;17(1):2909–13.
[47] TruffleSuite, Ganache-cli; 2019. https://github.com/trufflesuite/ganache-cli.
[48] EHPC, East Harbour Prosumers Community platform for sustainable energy use; 2019. < http://www.prosumers.nl/ > .
[49] Li N, Chen L, Low SH. Exact convex relaxation of OPF for radial networks using branch flow model. In: 2012 IEEE third international conference on smart grid communications (SmartGridComm), IEEE; 2012. p. 7–12.
[50] E.P.E. Netherlands, Day-ahead auction; 2019. http://www.apxgroup.com/trading-clearing/day-ahead-auction/.
[51] CBS, CBS StatLine - Verkeersprestaties personenauto's; kilometers, brandstofsoort, grondgebied; 2018. https://bit.ly/2OJtaCy.
[52] Gerritsma MK, AlSkaif TA, Fidder HA, van Sark WG. Flexibility of electric vehicle demand: analysis of measured charging data and simulation for the future. World Electric Veh J 2019;10(1):14.
[53] Mayer J. Current and future cost of photovoltaics. Long-term scenarios for market development, system prices and lcoe of utility-scale pv systems. https://www.ise.fraunhofer.de/content/dam/ise/de/documents/publications/studies/AgoraEnergiewende_Current_and_Future_Cost_of_PV_Feb2015_web.pdf.